

Contents lists available at ScienceDirect

Computer Aided Geometric Design

www.elsevier.com/locate/cagd



Interpolatory Catmull-Clark volumetric subdivision over unstructured hexahedral meshes for modeling and simulation applications



Jin Xie^a, Jinlan Xu^a, Zhenyu Dong^a, Gang Xu^{a,*}, Chongyang Deng^b, Bernard Mourrain^c, Yongjie Jessica Zhang^d

- ^a School of Computer Science and Technology, Hangzhou Dianzi University, Hangzhou, China
- ^b College of Science, Hangzhou Dianzi University, Hangzhou, China
- ^c Aromath, INRIA Sophia Antipolis, France
- ^d Department of Mechanical Engineering, Carnegie Mellon University, United States of America

ARTICLE INFO

Article history: Received 12 March 2020 Received in revised form 9 April 2020 Accepted 14 April 2020 Available online 22 April 2020

Kevwords:

Interpolatory volumetric subdivision Progressive-iterative approximation Volumetric material modeling Isogeometric analysis

ABSTRACT

Volumetric modeling is an important topic for material modeling and isogeometric simulation. In this paper, two kinds of interpolatory Catmull-Clark volumetric subdivision approaches over unstructured hexahedral meshes are proposed based on the limit point formula of Catmull-Clark subdivision volume. The basic idea of the first method is to construct a new control lattice, whose limit volume by the Catmull-Clark subdivision scheme interpolates vertices of the original hexahedral mesh. The new control lattice is derived by the local push-back operation from one Catmull-Clark subdivision step with modified geometric rules. This interpolating method is simple and efficient, and several shape parameters are involved in adjusting the shape of the limit volume. The second method is based on progressive-iterative approximation using limit point formula. At each iteration step, we progressively modify vertices of an original hexahedral mesh to generate a new control lattice whose limit volume interpolates all vertices in the original hexahedral mesh. The convergence proof of the iterative process is also given. The interpolatory subdivision volume has C^2 -smoothness at the regular region except around extraordinary vertices and edges. Furthermore, the proposed interpolatory volumetric subdivision methods can be used not only for geometry interpolation, but also for material attribute interpolation in the field of volumetric material modeling. The application of the proposed volumetric subdivision approaches on isogeometric analysis is also given with several examples.

© 2020 Elsevier B.V. All rights reserved.

1. Introduction

Volumetric representation describes the interior of an object in addition to its boundaries, which plays an important role in modeling and simulation applications. For example, volumetric modeling is required in advanced manufacturing technologies with heterogeneous materials, such as additive manufacturing of functionally graded material [Massarwi and Elber (2016)]. On the other hand, in three-dimensional isogeometric analysis [Lai et al. (2017)], volumetric modeling plays a

^{*} Corresponding author.

E-mail address: gxu@hdu.edu.cn (G. Xu).

key role as a geometric foundation for numerical simulation [Zhang et al. (2007), Xu et al. (2017)]. Trivariate NURBS solids [Xu et al. (2013a), Xu et al. (2013b), Xu et al. (2018), Xu et al. (2015), Xu et al. (2014), Pan et al. (2020), Pan et al. (2018), Massarwi et al. (2019)] and trivariate T-spline solids [Wang et al. (2012), Zhang et al. (2012), Wang et al. (2013), Liu et al. (2014), Wei et al. (2017a)] have been used as modeling and numerical tools in isogeometric modeling and analysis. However, because of their tensor–product structure, trivariate NURBS and T-spline solids have some limitations on the construction of analysis-suitable volumetric parameterizations from arbitrary complex geometries [Wei et al. (2017b), Wei et al. (2018), Chen et al. (2019)]. Hence, volumetric modeling for geometry with arbitrary topology is a key challenge to be addressed for material modeling and isogeometric analysis.

Subdivision is a simple and efficient technique for surface modeling in computer graphics, which can generate smooth surfaces from an input coarse control mesh with arbitrary topology [Catmull and Clark (1978)]. There are some related works on volumetric generalization of subdivision surfaces. However, most of them focus on approximating subdivision [Bajaj et al. (2002)]. There is very few work on interpolatory volumetric subdivision. In recent work, the authors proposed the limit point formula of Catmull-Clark volumetric subdivision [Xu et al. (2020)], which provides a key theoretical foundation for interpolatory Catmull-Clark volumetric subdivision.

In this paper, two kinds of interpolatory Catmull-Clark volumetric subdivision approaches over unstructured hexahedral meshes are proposed based on the limit point formula of Catmull-Clark subdivision volume. Main contributions of this paper can be summarized as follows:

- A simple and efficient interpolatory Catmull-Clark volumetric subdivision approach by the local push-back operation is proposed, and several shape parameters are involved in adjusting the limit volumes.
- A new interpolatory Catmull-Clark volumetric subdivision approach based on the progressive-iterative approximation is proposed. The convergence of the iterative process is also proven.
- The applications of the proposed interpolatory subdivision methods for volumetric modeling with heterogeneous materials and isogeometric analysis of heat conduction and linear elasticity problems are also presented.

The rest of the paper is structured as follows. Section 2 describes some related work on interpolatory subdivision surfaces and subdivision volumes. Section 3 reviews the Catmull-Clark volumetric subdivision rules and the corresponding limit point formula. The interpolatory Catmull-Clark volumetric subdivision based on the push-back operation is presented in Section 4. Section 5 describes the interpolatory Catmull-Clark volumetric subdivision based on progressive iterative approximation. Some comparison examples and applications in volumetric material modeling and isogeometric analysis are given in Section 6. Finally, we conclude this paper and outline future work in Section 7.

2. Related work

Interpolatory subdivision surface. Interpolatory subdivision surface can mainly be split into two categories. In the first one, the subdivision schemes consistently contain the old vertices in the refined mesh after each subdivision operation. Obviously, the limit surface generated in this way will contain all the original vertices. Butterfly scheme [Dyn et al. (1990)] and Kobbelt's scheme [Kobbelt (1996)] both fall into this category. Li et al. proposed a method for directly deducing new interpolation subdivision masks from the corresponding approximation subdivision masks [Kobbelt (1996)]. A unified interpolatory subdivision scheme is proposed for quadrilateral meshes based on local refinement operations in a way similar to that for approximating schemes generalizing splines of an arbitrarily high-order continuity in [Deng and Ma (2013)]. Another idea to generate a subdivision surface interpolating vertices of an input control mesh is to employ approximating subdivision schemes by adjusting vertices of the original control mesh. Halstead et al. [Halstead et al. (1993)] proposed a method by building a global linear system with some fairness constraints to make the limit surface interpolate vertices of the given control mesh. The push-back method was firstly proposed in [Maillot and Stam (2001)] to deal with the shrinkage issue of approximating subdivision schemes. Deng and Yang [Deng and Yang (2010)] applied this idea to the Catmull-Clark surface subdivision scheme to derive an interpolation scheme based on the explicit limit point formula. Progressive-iterative approximation (PIA for short) and weighted PIA have been used for constructing interpolatory subdivision surfaces by adjusting the control mesh iteratively [Chen et al. (2008), Cheng et al. (2009), Deng and Ma (2012)]. However, since the PIA method requires the explicit limit point formula to realize the interpolation, currently there is no related work on interpolatory volumetric subdivision based on PIA. Subdivision surfaces have also been used broadly in design and isogeometric analysis [Cirak et al. (2000), Pan et al. (2014), Pan et al. (2016)]. Truncation mechanism has been applied to Catmull-Clark subdivision to support local refinement [Wei et al. (2015), Wei et al. (2016)], and a hybrid non-uniform recursive subdivison scheme was developed to support isogeometric analysis with improved convergence rate [Li et al. (2019)].

Subdivision volume. Compared with subdivision surfaces, much less work has been done on volumetric subdivision. The first subdivision solid scheme was proposed by Joy and Maccracken in [MacCracken and Joy (1996)], which refines a volume mesh into a region of three-dimensional space. Bajaj et al. proposed a volumetric extension of the Catmull-Clark subdivision surface and analyzed the smoothness property [Bajaj et al. (2002)]. A new volumetric subdivision scheme based on Box splines was developed in [Chang et al. (2002)]. Chang et al. also presented an interpolating scheme for recursive subdivision of meshes organized around octet-truss structures [Chang et al. (2003)]. A natural generalization of the butterfly subdivision from 2D surface to 3D volume was proposed in [McDonnell et al. (2004)] as a novel interpolating volumetric scheme. In

the field of scientific visualization, an interactive visualization framework was proposed by using radial basis functions with subdivision volumes [McDonnell et al. (2007)]. Lin et al. proposed a constrained volume iterative fitting algorithm to fill a triangular mesh with an all-hex volume mesh [Lin et al. (2015)]. In that paper, they fit the boundary of the initial all-hex mesh to the given triangular mesh by iteratively adjusting the boundary mesh vertices, and the movements of the boundary mesh vertices are diffused to the inner all-hex mesh vertices in each iteration without the application of limit point formula. As an emerging application, isogeometric analysis based on approximation Catmull-Clark subdivision volumes were proposed in [Burkhart et al. (2010)], which can achieve a unified representation of geometric modeling and physical simulation. In this paper, two kinds of interpolatory Catmull-Clark volumetric subdivision approaches over unstructured hexahedral meshes are proposed based on the explicit limit point formula, and their application in volumetric material modeling and isogeometric analysis are also illustrated.

3. Catmull-Clark volumetric subdivision and limit point formula

Catmull-Clark volumetric subdivision is an volumetric extension of Catmull-Clark surface subdivision. Denote \hat{M}^0 the initial control lattice and \hat{M}^i the hex-mesh obtained after i steps of Catmull-Clark volumetric subdivision. Let e_k^i , f_k^i , c_k^i be the edge point, the face point and the cell point of a vertex in \hat{M}^i . The Catmull-Clark volumetric subdivision rules for unstructured hexahedral mesh with arbitrary topology can be described as the following five steps:

Step.1 For each cell, insert a cell point (on the centroid) c_k^i , which is the average of all vertices of this cell. Step.2 For each face, insert a face point f_k^i , which is derived from

$$f^{i+1} = \frac{c_1^i + c_2^i + 2A}{4} \tag{1}$$

where c_1^i and c_2^i are the cell points of two adjacent cells of this face, and A is the centroid of this face. Step.3 For each edge, insert an edge point, which is derived by

$$e^{i+1} = \frac{C_{avg} + 2F_{avg} + M}{4} \tag{2}$$

where C_{avg} is the average of cell points of all the incident cells of this edge, F_{avg} is the average of the centroids of all the incident faces of this edge, and M is the midpoint of the edge.

Step.4 For each hexahedral cell, connect the cell points with all the face points, and connect all the face points with all incident edge points in this cell respectively. Then each hexahedral cell is divided into eight hexahedral cells, in which the cell points, the face points and the edge points are new vertices of \hat{M}^{i+1} .

Step.5 Update each original vertex according to

$$v^{i+1} = \frac{C_{avg} + 3F_{avg} + 3E_{avg} + v^i}{8} \tag{3}$$

where C_{avg} , F_{avg} , E_{avg} are the averages of the cell points, the face points and the edge points of all adjacent cells, faces and edges, and v^i is the original vertex.

The above steps define the new geometry and the topology connectivity of new vertices. With these steps, a series of refined hex-meshes will be produced, which eventually converges to a limit volume called the Catmull-Clark subdivision volume.

Catmull-Clark subdivision surface has an explicit limit formula [Halstead et al. (1993)], which plays an important role in theoretical analysis and application of subdivision surface. Recently, the authors proposed an explicit limit point formula of Catmull-Clark subdivision volumes [Xu et al. (2020)]. The main result is that the limit point v_i^{∞} of v^0 on \hat{M}^0 can be computed in the following explicit form:

$$v_i^{\infty} = \frac{16(n-2)v_i^1 + 4\sum_{j=1}^n m_j e_j^1 + 4\sum_{j=1}^{3(n-2)} f_j^1 + \sum_{j=1}^{2(n-2)} c_j^1}{30(n-2) + 4\sum_{j=1}^n m_j}$$
(4)

where n is the valence of an interior vertex v^i , m_i is the valence of the j-th adjacent edge of v_i , and

$$V_i^1 = \{v_i^1, e_1^1, ..., e_n^1, f_1^1, ..., f_{3(n-2)}^1, c_1^1, ..., c_{2(n-2)}^1\}$$

is the adjacency of v^i . e^i , f^i , c^i are the edge points, face points and cell points respectively after performing Catmull-Clark solid subdivision once.

In the following sections, based on this explicit limit point formula, two kinds of interpolatory Catmull-Clark volumetric subdivision approaches will be introduced.

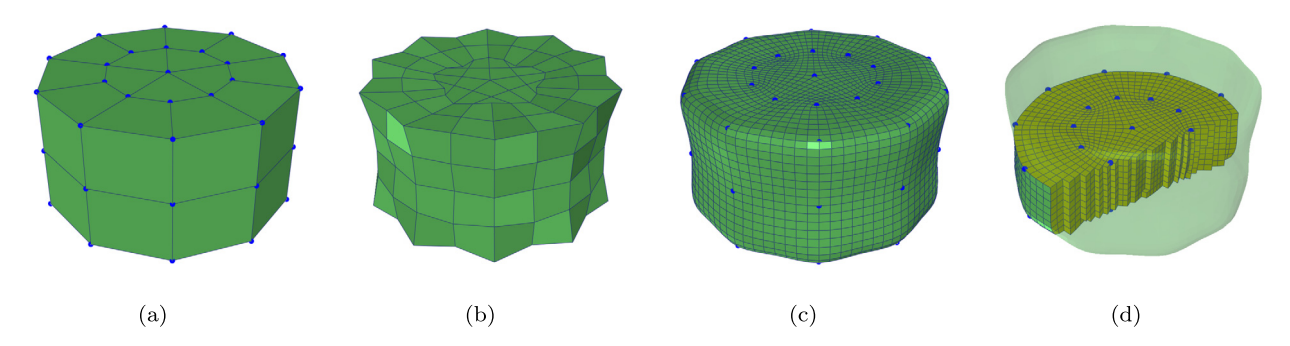


Fig. 1. Interpolatory Catmull-Clark volumetric subdivision example with the push-back method. (a) The original mesh; (b) new control lattices constructed by the push-back operation; (c) subdivision result after two levels of Catmull-Clark volumetric subdivision from the modified control lattice; (d) the interior view of the result.

4. Interpolatory Catmull-Clark volumetric subdivision with push-back operation

In this paper, we will introduce the interpolatory Catmull-Clark volumetric subdivision with the push-back operation. By using the limit point formula of Catmull-Clark subdivision volumes, from a given hexahedral control lattice, we can construct a new control lattice whose limit subdivision volume interpolates vertices of the original control lattice. Moreover, due to its local property, the interpolatory subdivision results can be obtained efficiently. By changing the shape parameters involved in this method, different subdivision volumes can be constructed to satisfy the interpolation condition.

Suppose that M^1 is the hexahedral control lattice obtained by performing one Catmull-Clark subdivision step on the initial hexahedral control lattice M^0 , V_i^1 on M^1 is the corresponding vertex of V_i^0 on M^0 . Then we define an increment as

$$\Delta_i^0 = V_i^0 - V_i^1. {5}$$

For each edge E_{ij} with end points V_i^0 and V_j^0 in M^0 , we can define

$$E' = \frac{1}{2}(V_i^0 + V_j^0) + \lambda_{ij}(\Delta_i^0 + \Delta_j^0), \quad 0 < \lambda_{ij} < 1$$
 (6)

as the edge point of this edge. Δ_i^0 and Δ_j^0 are the increments of two ending points respectively and λ_{ij} is a shape parameter, which can be used as a degree of freedom to construct different limit volumes.

For each face F in M^0 , we can define

$$F' = \frac{\sum_{j=1}^{4} V_j^0}{4} + 2\mu_F \sum_{j=1}^{4} \Delta_j^0, \quad 0 < \mu_F < 1$$
 (7)

as the face point of this face, in which Δ_j^0 is the increment for vertices on this face, where μ_F is also a shape parameter. Similarly, for each cell C in M^0 , we can define

$$C' = \frac{\sum_{j=1}^{8} V_j^0}{8} + 2\gamma_C \sum_{j=1}^{8} \Delta_j^0, \quad 0 < \gamma_C < 1$$
 (8)

as the cell point, in which Δ_j^0 is the increment of eight vertices of this cell. Here γ_C is a shape parameter influencing the final result.

In order to satisfy the interpolation condition, the original vertices of the control lattice should be set as the limit points, that is, $V_i^{\infty} = V_i^0$. Then we have a new hex-mesh with E', F', C' as above and the following vertices:

$$V' = \frac{[30(n-2) + 4\sum_{j=1}^{n} m_j]V_i^0 - 4\sum_{j=1}^{n} m_j E_j' - 4\sum_{j=1}^{3(n-2)} F_j' - \sum_{j=1}^{2(n-2)} C_j'}{16(n-2)}.$$
 (9)

After the above steps, now we can obtain a new hexahedral control lattice whose limit subdivision volume interpolates all the vertices V^0 of M^0 . From the new control lattice, we can obtain a limit volume interpolating the original control points by applying the Catmull-Clark volumetric subdivision rules.

Fig. 1 shows an interpolatory volume example with the push-back method. Fig. 1(a) is the original control lattice. Fig. 1(b) is the control lattice constructed by the push-back operation. Fig. 1(c) shows the volumetric subdivision results from the modified control lattice. Fig. 1(d) is the interior view of Fig. 1(c). We can find that the final subdivision volume interpolates the original control lattice exactly. Fig. 2 presents interpolatory volumetric subdivision examples with different shape parameters in the push-back method.

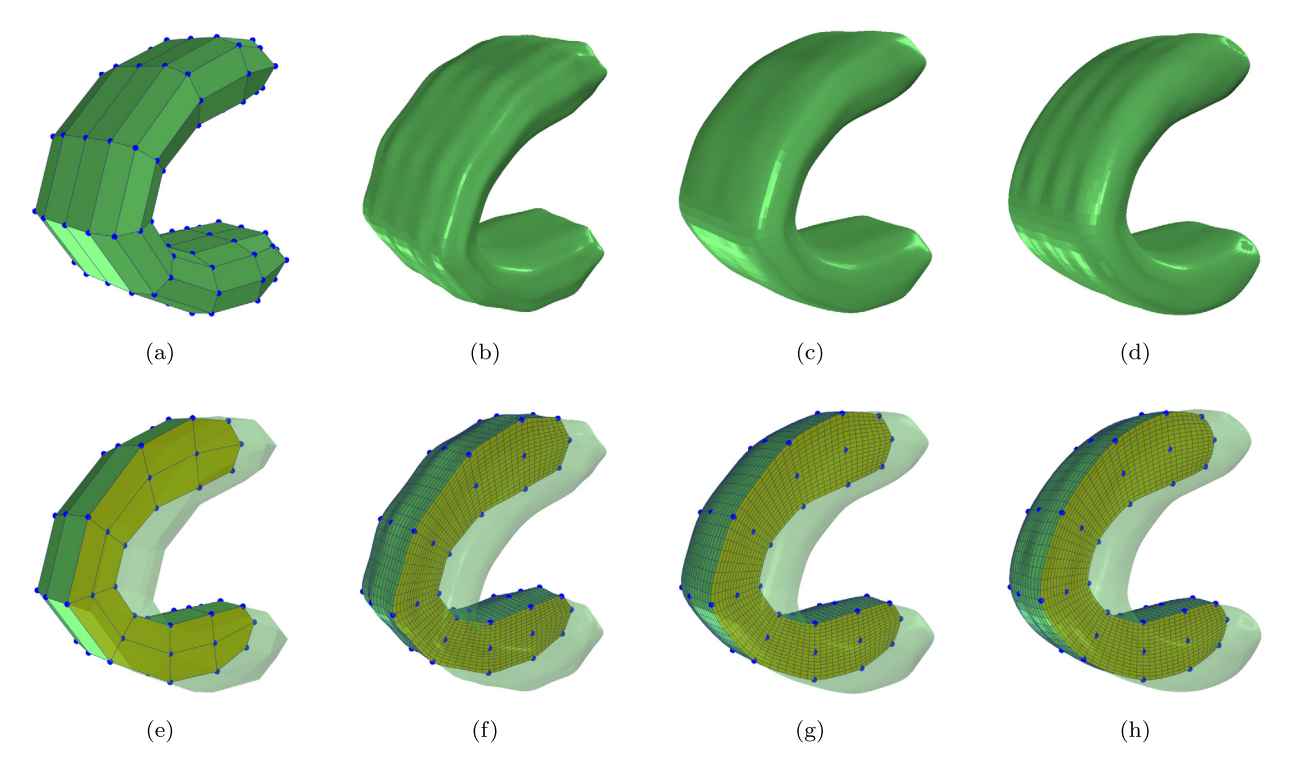


Fig. 2. Examples of the push-back method with different parameters. (a) and (e): The original mesh; (b) and (f): interpolatory subdivision volume with $\lambda_{ij} = 0.05$, $\mu_F = 0.05$ and $\gamma_C = 0.05$; (c) and (g): interpolatory subdivision volume with $\lambda_{ij} = 0.25$, $\mu_F = 0.125$ and $\gamma_C = 0.0625$; (d) and (h): interpolatory subdivision volume with $\lambda_{ij} = 0.25$, $\mu_F = 0.25$ and $\gamma_C = 0.25$.

5. Progressive interpolation using Catmull-Clark volume subdivision

Progressive-iterative approximation is an iterative method with clear geometric meaning, which was first proposed by Qi et al. [Qi et al. (1975)] and de Boor [de Boor (1979)]. A detailed review about progressive-iterative approximation was given in [Lin et al. (2018)]. In this paper, based on the limit point formula, we derive a volumetric interpolating scheme based on Catmull-Clark volumetric subdivision by using progressive-iterative approximation.

5.1. Interpolation process

Denote by \hat{M}^k the volumetric control lattice from the original volume mesh after k steps of modification. For each vertex v^k in \hat{M}^k , we compute its limit position of Catmull-Clark solid subdivision, namely v_{∞}^k , according to the limit point formula. Then the distance d^k between the counterpart of v^k in \hat{M}^k , namely v^0 , and v_{∞}^k can be computed as

$$d^k = v^0 - v_\infty^k. \tag{10}$$

Then we modify all $v^k \in \widehat{M}^k$ by adding d^k and get v^{k+1} by

$$v^{k+1} = v^k + d^k. \tag{11}$$

After several iterative steps, the final limit subdivision volume can achieve an interpolation of initial hexahedral control lattice. Fig. 3 shows an interpolatory volume example with the PIA method. Fig. 3(a)-3(d) show the iterative process of the control lattice, and Fig. 3(e)-3(h) illustrate the corresponding iterative process of the limit volumes, in which the blue points are vertices to be interpolated.

5.2. Convergence analysis

In this section, we will prove the convergence of the proposed PIA approach for Catmull-Clark subdivision volumes. Since the convergence of PIA on Catmull-Clark subdivision surface has been proved in [Chen et al. (2008)], we can firstly perform PIA on the boundary surface vertices of the volume mesh and fix them in the following steps. Then, by repeating the process (10)-(11), we can get a sequence of volume meshes \widehat{M}^k (k = 1, 2...). We want to prove that as k tends to infinity, \widehat{M}^k converges to the limit subdivision volume, which interpolates all the vertices in the original mesh \widehat{M}^0 .

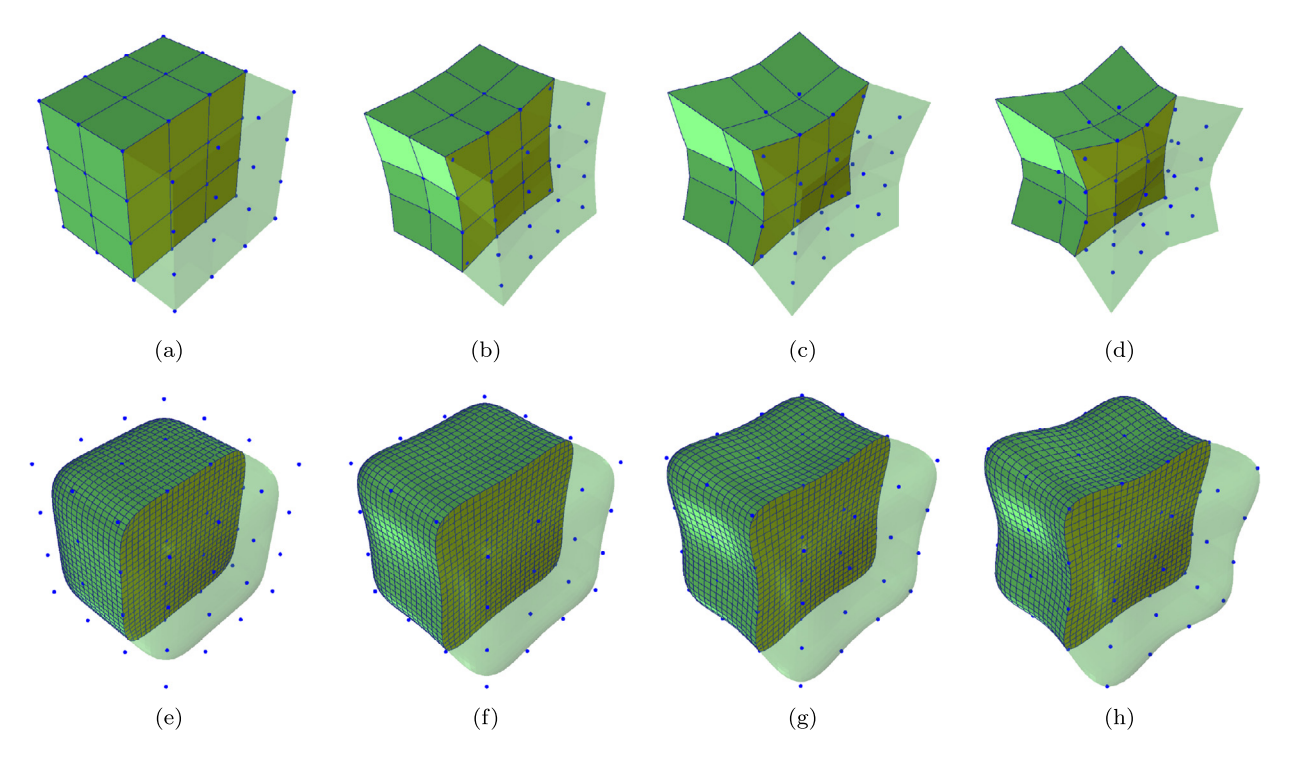


Fig. 3. Interpolatory volume example with the PIA method. (a): The original mesh; (b-d): new control lattices after one, three and ten PIA steps; (e-h): the corresponding iterative process of the limit volumes, in which the blue points are vertices of the original mesh.

The key to prove the convergence of \widehat{M}^k is to show that when k tends to infinity, d^k converges to zeros. For each interior vertex, we have

$$v_{\infty}^{k} = \frac{16(n-2)v^{k} + 4\sum_{j}m_{j}e_{j}^{k} + 4\sum_{j}f_{j}^{k} + \sum_{j}c_{j}^{k}}{30(n-2) + 4\sum_{j}m_{j}}.$$
(12)

By applying (12) to (10), we have

$$d^{k+1} = v_0 - \frac{16(n-2)v^{k+1} + 4\sum_{j} m_j e_j^{k+1} + 4\sum_{j} f_j^{k+1} + \sum_{j} c_j^{k+1}}{30(n-2) + 4\sum_{j} m_j}$$

$$= v_0 - \frac{16(n-2)v^k + 4\sum_{j} m_j e_j^k + 4\sum_{j} f_j^k + \sum_{j} c_j^k}{30(n-2) + 4\sum_{j} m_j}$$

$$- \frac{16(n-2)d^k + 4\sum_{j} m_j d_{e_j}^k + 4\sum_{j} d_{f_j^k}^k + \sum_{j} d_{c_j^k}^k}{30(n-2) + 4\sum_{j} m_j}$$

$$= d^k - \frac{16(n-2)d^k + 4\sum_{j} m_j d_{e_j}^k + 4\sum_{j} d_{f_j^k}^k + \sum_{j} d_{c_j^k}^k}{30(n-2) + 4\sum_{j} m_j}$$

$$(13)$$

in which $d^k = 0$ when it corresponds to a vertex on the surface.

Denote l as the number of vertices on the boundary surface, r as the number of all vertices in the given mesh. Equation (13) can be written in matrix form as

$$\begin{pmatrix} d_1^{k+1} \\ d_2^{k+1} \\ \dots \\ d_l^{k+1} \\ d_{l+1}^{k+1} \\ \dots \\ d_r^{k+1} \end{pmatrix} = (I - M) \begin{pmatrix} d_1^k \\ d_2^k \\ \dots \\ d_l^k \\ d_{l+1}^k \\ \dots \\ d_r^k \end{pmatrix} = (I - M)^{k+1} \begin{pmatrix} d_1^0 \\ d_2^0 \\ \dots \\ d_l^0 \\ d_{l+1}^0 \\ \dots \\ d_r^0 \end{pmatrix}$$

$$(14)$$

where $d_i^0 = 0$ (i = 1, 2, ..., l), I is the identity matrix of order r, M is a matrix with the following form:

$$M = \begin{pmatrix} 0 & 0 \\ M_1 & M_2 \end{pmatrix}, \tag{15}$$

$$M_{1} = \begin{pmatrix} \frac{4m_{ij}}{30(n_{l+1}-2)+4\sum_{j}m_{j}} & \cdots & \frac{4}{30(n_{l+1}-2)+4\sum_{j}m_{j}} & \cdots & \frac{1}{30(n_{l+1}-2)+4\sum_{j}m_{j}} & \cdots \\ \frac{4}{30(n_{l+j}-2)+4\sum_{j}m_{j}} & \cdots & \ddots & \ddots & \vdots \\ \vdots & & & \vdots & & \vdots & \ddots & \vdots \\ \frac{1}{30(n_{l+1}-2)+4\sum_{j}m_{j}} & \cdots & \cdots & \cdots & \cdots \end{pmatrix},$$

$$(16)$$

 $M_2 =$

$$\begin{pmatrix} \frac{16(n_{l+1}-2)}{30(n_{l+1}-2)+4\sum_{j}m_{j}} & \cdots & \frac{4m_{ij}}{30(n_{l+1}-2)+4\sum_{j}m_{j}} & \cdots & \frac{1}{30(n_{l+1}-2)+4\sum_{j}m_{j}} & \cdots \\ \vdots & & \ddots & & \\ \frac{4m_{ij}}{30(n_{l+i}-2)+4\sum_{j}m_{j}} & & \frac{16(n_{l+i}-2)}{30(n_{l+i}-2)+4\sum_{j}m_{j}} & & \vdots \\ \frac{4}{30(n_{l+j}-2)+4\sum_{j}m_{j}} & & \vdots & & \ddots \\ \vdots & & & & \ddots & \\ \frac{1}{30(n_{l+k}-2)+4\sum_{j}m_{j}} & & \ddots & & \\ \vdots & & & & \ddots & \\ \cdots & & & & \frac{16(n_{l+r}-2)}{30(n_{l+r}-2)+4\sum_{j}m_{j}} \end{pmatrix}$$

where n_i is the valence of the *i*-th vertex, and m_{ij} is the valence of the i-j edge.

Because $d_i^k = 0$ (i = 1, 2, ..., l) and $M_{ij} = 0$ (i, j = 1, 2, ..., l), proving that d^k converges to zero. The problem reduces to proving that the absolute value of each eigenvalue of the matrix (I - M') is less than 1, where $M' = M_2$. Furthermore, from [Chen et al. (2008), Cheng et al. (2009), Deng and Ma (2012)], we have the following similar proposition.

Proposition 1. Suppose that λ_i $(i=1,2,\ldots,r-l)$ are the eigenvalues of $M'=M_2$, if $\lambda_i>0$ $(i=1,2,\ldots,r-l)$, then the absolute value of each eigenvalue of the matrix (I-M') is less than 1.

In the above proposition, we suppose that the eigenvalues of M' are all positive. Hereafter, we have $\lambda_i > 0$ (i = 1, 2, ..., r - l). According to [Chen et al. (2008)], we know that the eigenvalues of the product of two positive definite matrices are positive. Hence, we can first decompose the matrix M' into the product of A and B, in which

$$A = \begin{pmatrix} \frac{1}{30(n_{l+1}-2)+4\sum_{j}m_{j}} & 0 & \cdots & 0 \\ 0 & \frac{1}{30(n_{l+2}-2)+4\sum_{j}m_{j}} & \cdots & 0 \\ \vdots & & \ddots & & \\ 0 & & \cdots & \frac{1}{30(n_{r}-2)+4\sum_{j}m_{j}} \end{pmatrix},$$

$$B = \begin{pmatrix} 16(n_{l+1}-2) & \cdots & 4m_{lj} & \cdots & 4 & \cdots & 1 & \cdots \\ \vdots & \ddots & & & & \\ 4m_{lj} & 16(n_{l+i}-2) & & & & \\ \vdots & & & & & \\ 4 & & \ddots & & & \\ \vdots & & & & & \\ 1 & & & & \ddots & & \\ \end{pmatrix}.$$

$$(18)$$

Obviously, *A* is diagonal and all elements on the diagonal line are positive, thus it is positive definite. Now the only thing that we need to prove is that the matrix *B* is positive definite.

Proposition 2. *Matrix B in* (19) *is positive definite.*

Proof. Matrix *B* is positive definite if and only if the corresponding quadratic form is positive for any non-zero vector $X = (x_{l+1}, x_{l+2}, \dots, x_r)$:

$$f(x_{l+1}, x_{l+2}, \dots, x_r) = X^T B X > 0.$$
 (20)

We can see that if vertices v_i and v_j are adjacent, then $b_{ij} = b_{ji} = 4m_{ij}$. If they are not adjacent but lie in the same face, then $b_{ij} = b_{ji} = 4$. If they do not lie on the same face but lie in the same cell, then $b_{ij} = b_{ji} = 1$. Thus we can get

$$f(x_{l+1}, x_{l+2}, \dots, x_r) = \sum_{i=l+1}^r 16(n_i - 2)x_i^2 + \sum_{e_{ij}} 8m_{ij}x_ix_j + \sum_{f_{ij}} 8x_ix_j + \sum_{c_{ij}} 2x_ix_j$$
(21)

where e_{ij} , f_{ij} and c_{ij} range through all edges, all diagonals of each face and all diagonals of each cell inside the volume (we do not include those on the surface).

In order to prove that (21) is positive, we construct the following equation. For all edges of the mesh, when x_i corresponds to a surface vertex, set it to zero. Then we obtain

$$\sum_{e_{ij}} m_{ij} (x_i + x_j)^2 = \sum_{l+1}^r \sum_{i} m_j x_i^2 + \sum_{e_{ij}} 2m_{ij} x_i x_j$$
(22)

where the sum is taken for all edges e_{ij} of the mesh (including surface edges). For all faces, similarly we have

$$\sum_{f_{ijpq}} (x_i + x_j + x_p + x_q)^2 = \sum_{l+1}^{r} 3(n_i - 2)x_i^2 + \sum_{e_{ij}} 2m_{ij}x_ix_j + \sum_{g_{ij}} 2x_ix_j$$
(23)

where g_{ij} means a pair of diagonal vertices on a given face. For all cells, we have

$$\sum_{c_{ijpquxyz}} (x_i + x_j + x_p + x_q + x_u + x_x + x_y + x_z)^2 = \sum_{l+1}^r 2(n_i - 2)x_i^2 + \sum_{e_{ij}} 2m_{ij}x_ix_j + \sum_{g_{ij}} 4x_ix_j + \sum_{h_{ij}} 2x_ix_j$$
 (24)

where h_{ii} means a pair of diagonal vertices on a given cell.

By applying (22)-(24) to (21), we have

$$f(x_{l+1}, x_{l+2}, \dots, x_r) = \sum_{c_{ijpquxyz}} (x_i + x_j + x_p + x_q + x_u + x_x + x_y + x_z)^2$$

$$+ 2 \sum_{f_{ijpq}} (x_i + x_j + x_p + x_q)^2 + \sum_{e_{ij}} m_{ij} (x_i + x_j)^2 + \sum_{i=l+1}^r \left[8 (n_i - 2) - \sum_j m_j \right] x_i^2.$$
(25)

For each interior edge, m is equal to the number of adjacent cells. When computing $\sum_j m_j$ for a vertex, each adjacent cell will be counted three times because it must have three edges adjacent to the vertex. For each vertex, the number of adjacent cells is $2(n_i - 2)$. Thus we have

$$\sum_{i} m_{j} = 6 (n_{i} - 2). \tag{26}$$

Substituting (26) into (25), we can obtain

$$f(x_{l+1}, x_{l+2}..., x_r) = \sum_{c_{ijpquuryz}} (x_i + x_j + x_p + x_q + x_u + x_x + x_y + x_z)^2 + 2\sum_{f_{ijnq}} (x_i + x_j + x_p + x_q)^2 + \sum_{e_{jj}} m_{ij} (x_i + x_j)^2 + \sum_{i=l+1}^r 2(n_i - 2)x_i^2 > 0.$$
(27)

Equation (27) shows that $f(x_{l+1}, x_{l+2}, \dots, x_r)$ is always positive for any non-zero vector X. The above proof shows that B is positive definite, and the convergence of PIA on Catmull-Clark subdivision solid is proved. \Box

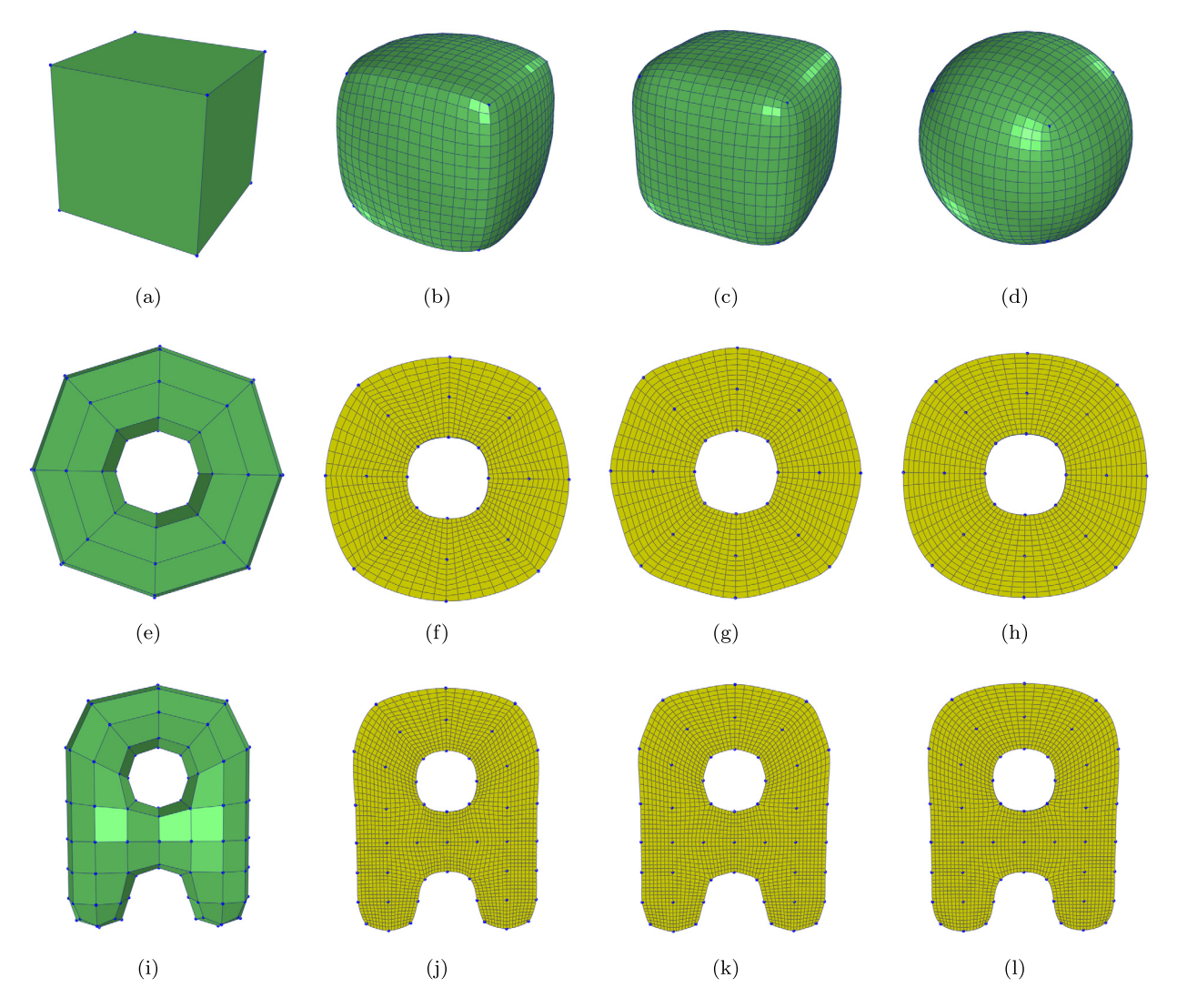


Fig. 4. Comparison examples. From left to right: The input hexahedral mesh; the butterfly interpolatory subdivision method; the push-back method; and the PIA method.

6. Examples and applications

In this section, we will compare the proposed interpolatory subdivision schemes with the butterfly volumetric subdivision approach [McDonnell et al. (2004)], then we will present the applications of the proposed interpolatory subdivision methods for volumetric modeling with heterogeneous materials and isogeometric analysis of heat conduction and linear elasticity problems.

6.1. Comparison

The proposed interpolatory volumetric subdivision method can achieve a limit volumetric geometry with C^2 -continuity at regular part. McDonnell et al. has proposed a volumetric subdivision algorithm based on the well-known Lagrange polynomials, which is C^1 continuous at regular part. It can be seen as a natural generalization of the butterfly subdivision surface scheme to the volumetric case. Fig. 4 presents three examples for the comparison of the butterfly method, the push-back method and the PIA approach. From these modeling examples, we can find that the PIA-based interpolatory volumetric subdivision results are much smoother than the butterfly volumetric subdivision results. From the cross-section of these models as shown in Fig. 4(f)-4(h) and Fig. 4(j)-4(l), we can find that the PIA method can also achieve smoother interior mesh structure than the butterfly subdivision approach. Another comparison example is shown in Fig. 5(b)-5(d).

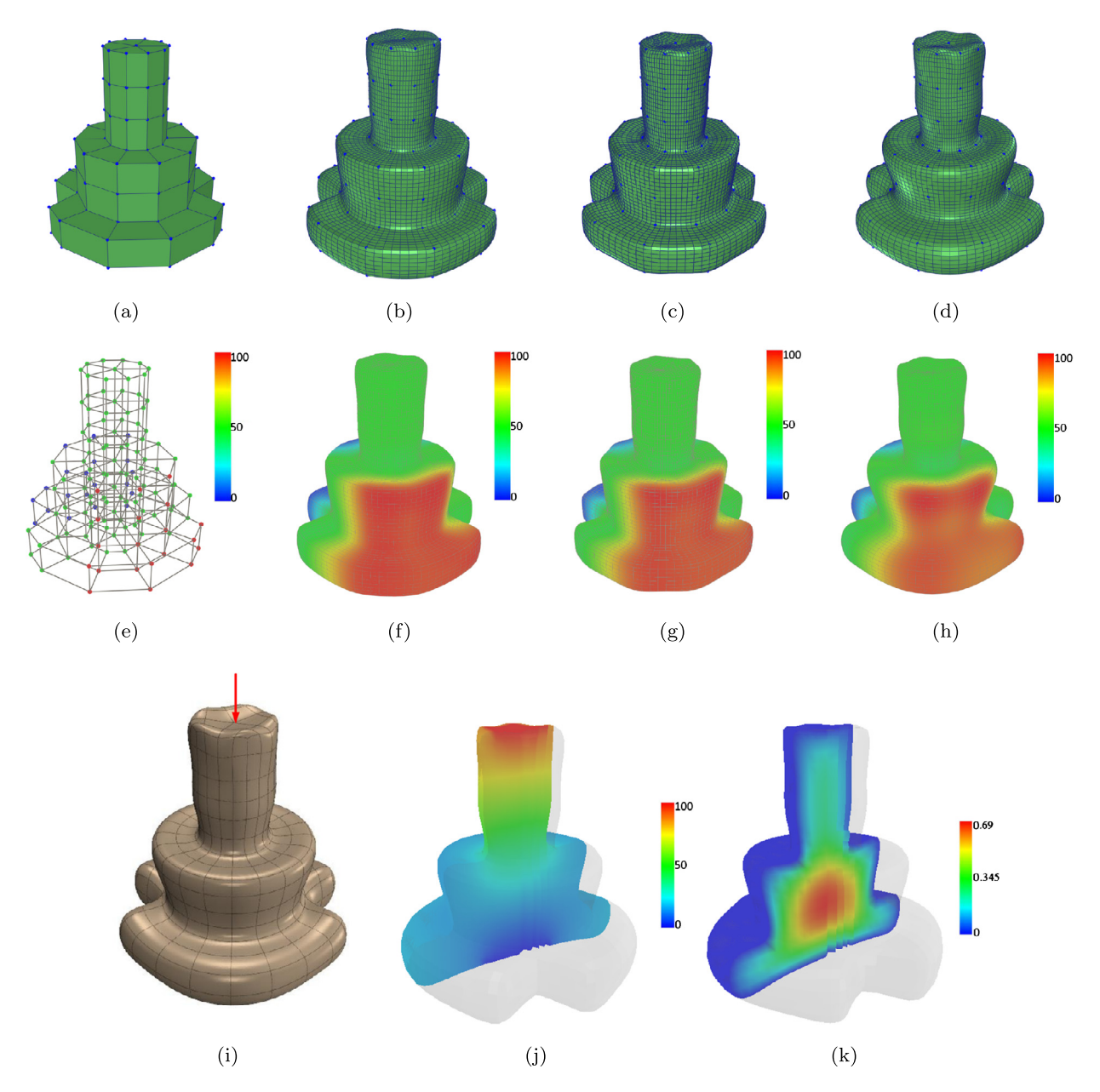


Fig. 5. Comparison examples. (a-h): The input hexahedral mesh; the butterfly interpolatory subdivision method; the push-back method; and the PIA method. Blue, green and red vertices in (e) are assigned with material value 0, 50 and 100 respectively. (f-h): The corresponding material description over (b), (c) and (d) geometry, respectively. (i): Boundary condition for linear elasticity simulation on the interpolatory subdivision volume with the PIA method in (d); (j): IGA results for linear elasticity simulation with boundary condition in (i); (k): IGA results for heat conduction simulation.

6.2. Application in volumetric modeling with heterogeneous materials

Multi-material 3D printers are more and more popular for additive manufacturing, and the research on heterogeneous materials, especially the functionally graded material objects, is a hot topic in the field of intelligent manufacturing. The proposed interpolatory volumetric subdivision methods can be used not only for geometry interpolation, but also for material attribute interpolation in the field of volumetric material modeling with heterogeneous materials, which is a major benefit of our volumetric subdivision scheme.

Fig. 6 shows a volumetric geometry and the material interpolation process by the interpolatory volumetric subdivision approach based on PIA, and the final volumetric material object can interpolate the material values at vertices of the input control lattice. Fig. 5(e)-5(h), Fig. 8(d)-8(i) and Fig. 9(c)-9(e) illustrate several volumetric material modeling examples with heterogeneous material properties associated with geometry. In these examples, different material densities are assigned to

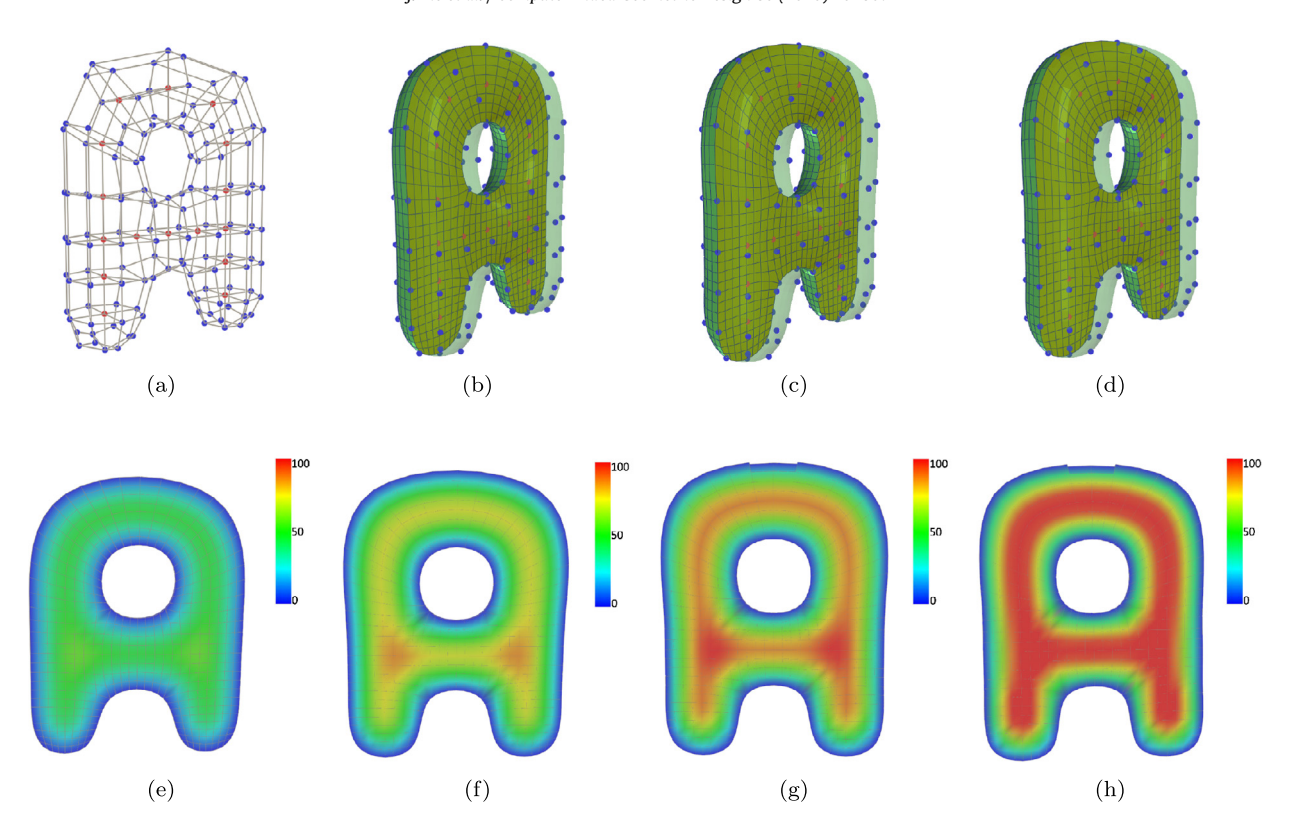


Fig. 6. Volumetric geometry and material interpolation by the interpolatory volumetric subdivision approach based on PIA. (a): The original control lattice with different material values at vertices, where blue vertices have material value 0 and red vertices have material value 100; (b) - (d): volumetric subdivision results after one, three and ten PIA operations; (e): material distribution of subdivision volumes after two Catmull-Clark volumetric subdivision steps; (f) - (h): the corresponding material distribution after one, three and ten PIA operations with respect to (b) - (d).

different control points. By using our interpolatory volumetric approach, we can blend different densities smoothly and the resulting functionally graded material object can interpolate the material density at each control point exactly.

6.3. Application in isogeometric analysis

The proposed interpolatory volumetric subdivision methods have the following advantages for isogeometric analysis: (1) easy for imposing Dirichlet boundary conditions; (2) multi-resolution property; and (3) representation of complex geometry with arbitrary topology. Moreover, volumetric subdivision methods provide explicit regular shape functions for isogeometric application over complex geometry with arbitrary topology. In this paper, we also implement the isogeometric analysis framework with the proposed interpolatory volumetric subdivision for three-dimensional linear elasticity and heat conduction problems.

As an illustration problem, we consider the following three-dimensional heat conduction problem:

$$\begin{cases} -\Delta T(\mathbf{x}) = f(\mathbf{x}) & \text{in } \Omega \subset \mathbb{R}^3 \\ T(\mathbf{x}) = 0 & \text{on } \partial \Omega \end{cases}$$
 (28)

where Δ is the Laplacian operator, Ω is the computational domain represented by the interpolatory Catmull-Clark subdivision volume, $T(\mathbf{x})$ is the unknown heat field, and $f(\mathbf{x})$ is the heat source function.

The IGA approximation of (28) is to find the numerical solution T^h such that

$$\iint\limits_{\Omega} \nabla T^h \cdot \nabla v dx dy = \iint\limits_{\Omega} f \cdot v dx dy, \tag{29}$$

in which v is a test function. Each control point \mathbf{P}_i is associated with a basis function ϕ_i . In isogeometric framework, the solution field T^h has the following form

$$T^{h} = \sum_{j=1}^{n} \phi_{j} T_{j}^{h}, \tag{30}$$

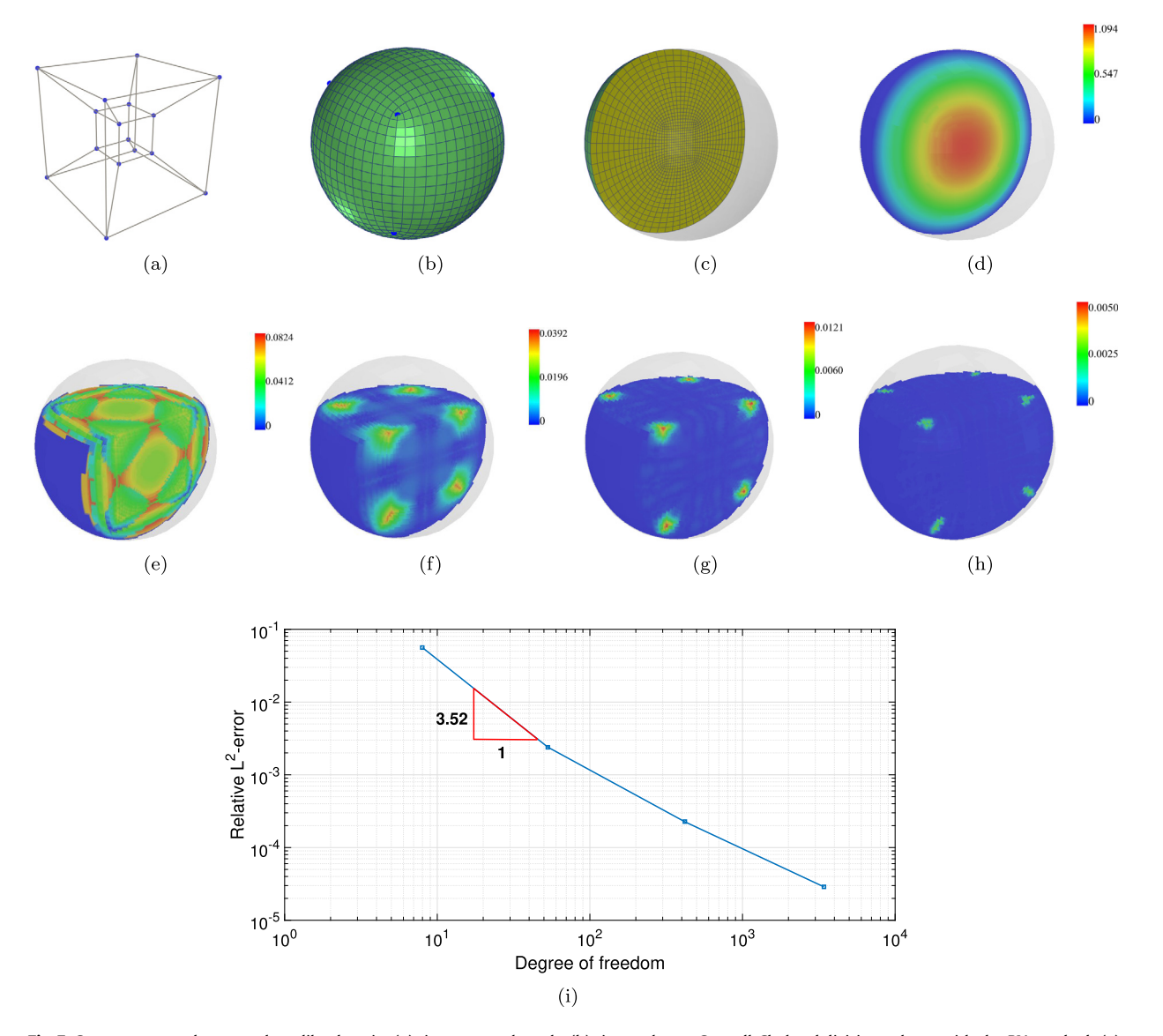


Fig. 7. Convergence study on a sphere-like domain. (a): input control mesh; (b): interpolatory Catmull-Clark subdivision volume with the PIA method; (c): the interior view of (b); (d): reference solution to heat conduction problems; (e): error colormap of numerical solution on the level-0 subdivision volume; (f): error colormap of numerical solution on the level-1 subdivision volume; (g): error colormap of numerical solution on the level-2 subdivision volume; (h): error colormap of numerical solution on the level-3 subdivision volume; (ii): convergence rate of relative L_2 error vs the number of degrees of freedom.

in which T_j^h is the unknown control variable [Pan et al. (2016, 2014)]. Then the numerical approximation problem (29) can be rewritten as

$$\sum_{j=1}^{n} T_{j}^{h} \iint_{\Omega} \nabla \phi_{j} \cdot \nabla \phi_{i} dx dy = \iint_{\Omega} f \cdot \phi_{i} dx dy, \quad i = 1, \dots, n.$$
(31)

Then we can obtain a linear system with unknown vector T,

$$KT = b$$
,

in which \mathbf{K} is the stiffness matrix and \mathbf{b} is the load vector described as

$$\mathbf{K} = \iint\limits_{\Omega} \nabla \phi_j \cdot \nabla \phi_i \mathrm{d}x \mathrm{d}y \quad \text{and} \quad \mathbf{b} = \iint\limits_{\Omega} f \cdot \phi_i \mathrm{d}x \mathrm{d}y. \tag{32}$$

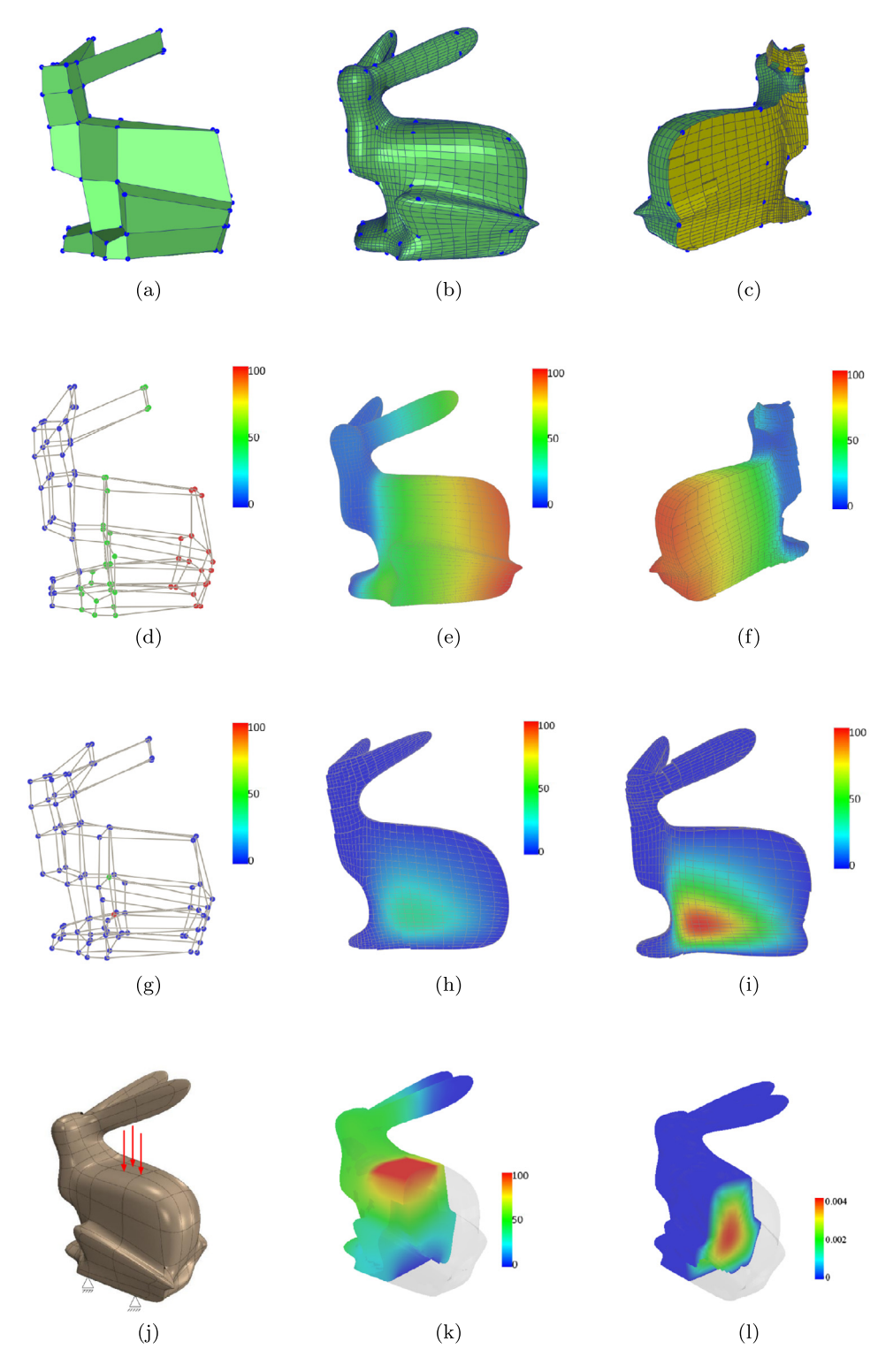


Fig. 8. Bunny model. (a): The original mesh; (b): interpolatory volumetric subdivision result with the PIA method; (c): the interior view of (b); (d): the original control lattice with different material values, where blue, green and red correspond to 0, 50 and 100, respectively; (e) and (f): material distribution of the interpolatory subdivision solids by the PIA method; (g) the original control lattice with another set of material values at vertices; (h) material distribution of approximation Catmull-Clark subdivision volume with input (g); (i) material distribution of interpolatory Catmull-Clark subdivision volume with input (g); (j): boundary condition for linear elasticity simulation; (k): IGA results for linear elasticity simulation with boundary condition (j); (l): IGA results for leat conduction simulation.

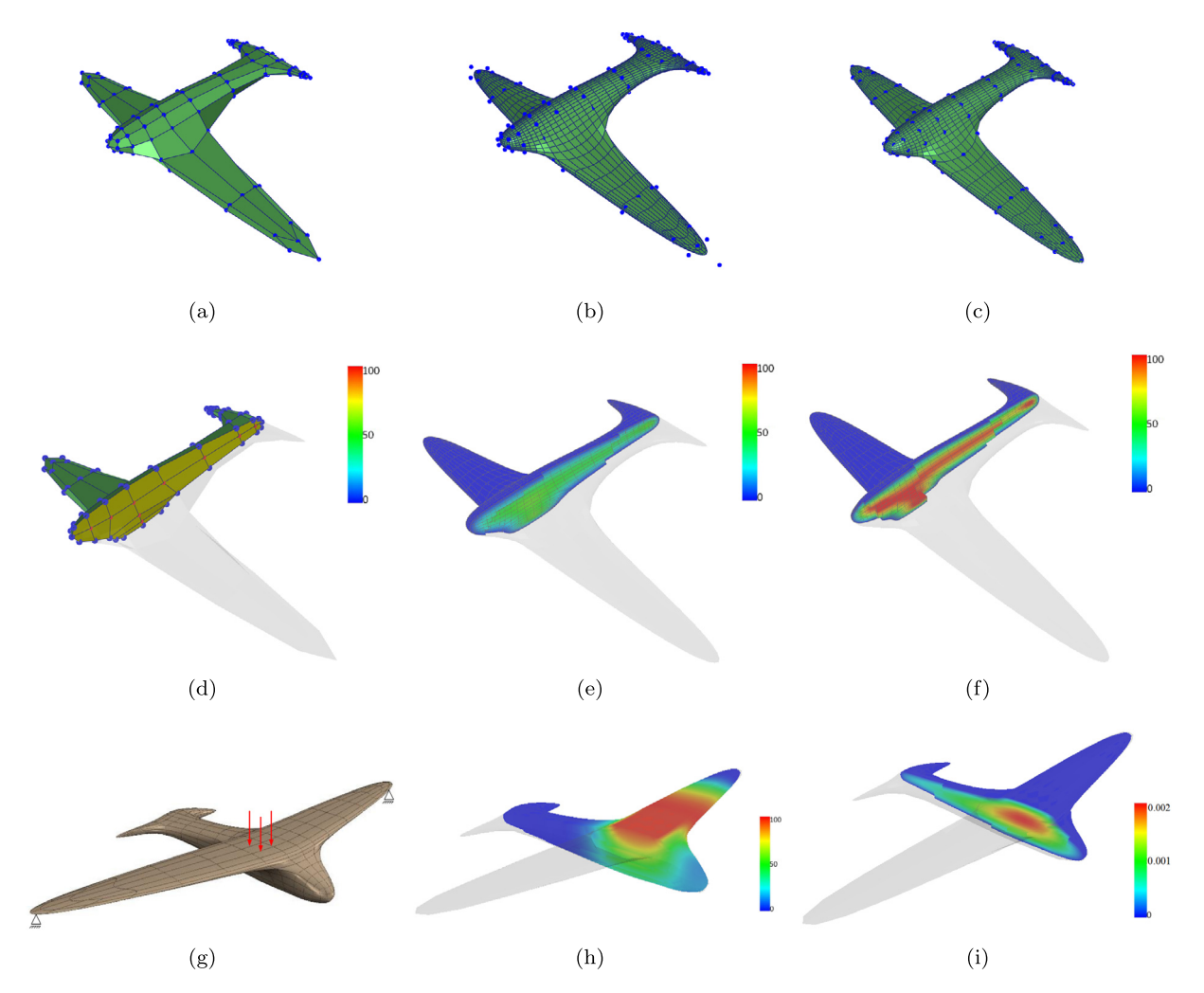


Fig. 9. Airplane model. (a): Input control lattice; (b): Catmull-Clark subdivision volume after three subdivision steps; (c): interpolatory Catmull-Clark subdivision volume after three subdivision steps with the PIA method; (d): the original control lattice with different material values at vertices, where blue vertices have material value 0 and red vertices have material value 100; (e): material distribution of approximation Catmull-Clark subdivision volume after three subdivision steps; (f): material distribution of interpolatory Catmull-Clark subdivision volume after three subdivision steps; (g): boundary condition for linear elasticity simulation; (h): IGA results for linear elasticity simulation with boundary condition (g); (i): IGA results for heat conduction simulation.

The stiffness matrix **K** and the load vector **b** over each element are evaluated by using three-dimensional Gauss-Legendre quadrature on the limit representation of the interpolatory Catmull-Clark subdivision volume. For the evaluation at the sampling points of the Gauss-Legendre quadrature, direct computation with cubic uniform B-spline basis functions is used for regular elements; for irregular elements, an approach based on diagonalization of the subdivision matrix is used to evaluate subdivision volumes at arbitrary parameter values [Stam (1998); Burkhart et al. (2010)].

For the convergence study of the IGA framework with interpolatory Catmull-Clark subdivision volumes, a heat conduction example of a sphere-like domain is presented in Fig. 7. The initial level-0 hex-mesh in Fig. 7(a) is subdivided three times to analyze the convergence, and the corresponding numerical error is computed with respect to a reference solution, which is solved with the level-4 hex-mesh as shown in Fig. 7(d). After performing volumetric subdivision steps and IGA solving, we can find that the numerical error is concentrated in regions around irregular edges and vertices as shown in Fig. 7(e)-7(h). Moreover, extraordinary edges and vertices also decrease the convergence rate as shown in Fig. 7(i). The convergence rate is sub-optimal at 3.52 for the relative L_2 error.

Fig. 5(i)-5(j), Fig. 8(j)-8(k) and Fig. 9(f)-9(h) illustrate several isogeometric simulation results for heat conduction and linear elasticity problems on complex geometry respectively.

7. Conclusion

With the help of limit point formula, two new methods are proposed to construct Catmull-Clark subdivision volumes that interpolate vertices of a given hex-mesh with arbitrary topology. The first method is based on the push-back operation,

and the second method is based on progressive-iterative approximation with convergence proof. Some comparisons with examples are given, and applications in volumetric material modeling and isogeometric analysis are also presented to show the effectiveness of the proposed methods.

For the research on volumetric subdivision, there are still a few key issues to be addressed. Compared with subdivision surfaces, the extension of the subdivision scheme to higher dimensions is not trivial, such as the smoothness property and local-refinement theory, which will be our future research topics.

Declaration of competing interest

The authors declare that they have no known competing financial interests or personal relationships that could have appeared to influence the work reported in this paper.

Acknowledgement

The authors thank the anonymous reviewers for providing constructive suggestions and comments, that contributed to highly improve this work. The authors appreciate the joint support for this project by the National Natural Science Foundation of China (Grant Nos. 61761136010, 61772163, 61872121), the Science Challenge Project (Grant No. TZ2016002), and the NSFC-Zhejiang Joint Fund for the Integration of Industrialization and Informatization (Grant No. U1909210).

References

Bajaj, C., Schaefer, S., Warren, J., Xu, G., 2002. A subdivision scheme for hexahedral meshes. Vis. Comput. 18, 343-356.

de Boor, C., 1979. How does Agee's smoothing method work. In: Proceedings of Army Numerical Analysis and Computers Conference, ARO Report, pp. 79–83. Burkhart, D., Hamann, B., Umlauf, G., 2010. Iso-geometric finite element analysis based on Catmull-Clark subdivision solids. Comput. Graph. Forum 29, 1575–1584

Catmull, E., Clark, J., 1978. Recursively generated B-spline surfaces on arbitrary topological meshes. Comput. Aided Des. 10, 350-355.

Chang, Y.S., McDonnell, K.T., Qin, H., 2002. A new solid subdivision scheme based on Box splines. In: Proceedings of the Seventh ACM Symposium on Solid Modeling and Applications, pp. 226–233.

Chang, Y.S., McDonnell, K.T., Qin, H., 2003. An interpolatory subdivision for volumetric models over simplicial complexes. In: Shape Modeling International, pp. 143–152.

Chen, L., Xu, G., Wang, S., Shi, Z., Huang, J., 2019. Constructing volumetric parameterization based on directed graph simplification of ℓ1 polycube structure from complex shapes. Comput. Methods Appl. Mech. Eng. 351, 422–440.

Chen, Z., Luo, X., Tan, L., Ye, B., Chen, J., 2008. Progressive interpolation based on Catmull-Clark subdivision surfaces. In: Computer Graphics Forum. Wiley Online Library, pp. 1823–1827.

Cheng, F.H.F., Fan, F.T., Lai, S.H., Huang, C.L., Wang, J.X., Yong, J.H., 2009. Loop subdivision surface based progressive interpolation. J. Comput. Sci. Technol. 24, 39–46.

Cirak, F., Ortiz, M., Schroder, P., 2000. Subdivision surfaces: a new paradigm for thin-shell finite-element analysis. Int. J. Numer. Methods Eng. 47, 2039–2072. Deng, C., Ma, W., 2012. Weighted progressive interpolation of Loop subdivision surfaces. Comput. Aided Des. 44, 424–431.

Deng, C., Ma, W., 2013. A unified interpolatory subdivision scheme for quadrilateral meshes. ACM Trans. Graph. 32, 23.

Deng, C., Yang, X., 2010. A simple method for interpolating meshes of arbitrary topology by Catmull-Clark surfaces. Vis. Comput. 26, 137-146.

Dyn, N., Levine, D., Gregory, J.A., 1990. A butterfly subdivision scheme for surface interpolation with tension control. ACM Trans. Graph. 9, 160-169.

Halstead, M., Kass, M., DeRose, T., 1993. Efficient, fair interpolation using Catmull-Clark surfaces. In: Proceedings of the 20th Annual Conference on Computer Graphics and Interactive Techniques. ACM, pp. 35–44.

Kobbelt, L., 1996. Interpolatory subdivision on open quadrilateral nets with arbitrary topology. In: Computer Graphics Forum. Wiley Online Library, pp. 409–420.

Lai, Y., Zhang, Y.J., Liu, L., Wei, X., Fang, E., Lua, J., 2017. Integrating CAD with Abaqus: a practical isogeometric analysis software platform for industrial applications. Comput. Math. Appl. 74, 1648–1660.

Li, X., Wei, X., Zhang, Y.J., 2019. Hybrid non-uniform recursive subdivision with improved convergence rates. Comput. Methods Appl. Mech. Eng. 352, 606–624.

Lin, H., Maekawa, T., Deng, C., 2018. Survey on geometric iterative methods and their applications. Comput. Aided Des. 95, 40-51.

Lin, H., Sinan, J., Hongwei, L., Qun, J., 2015. Quality guaranteed all-hex mesh generation by a constrained volume iterative fitting algorithm. Comput. Aided Des. 67–68, 107–117.

Liu, L., Zhang, Y., Hughes, T.J., Scott, M.A., Sederberg, T.W., 2014. Volumetric T-spline construction using Boolean operations. Eng. Comput. 30, 425–439.

MacCracken, R., Joy, K.I., 1996. Free-form deformations with lattices of arbitrary topology. In: Proceedings of the 23rd Annual Conference on Computer Graphics and Interactive Techniques. ACM, pp. 181–188.

Maillot, J., Stam, J., 2001. A unified subdivision scheme for polygonal modeling. In: Computer Graphics Forum. Wiley Online Library, pp. 471–479.

Massarwi, F., Antolin, P., Elber, G., 2019. Volumetric untrimming: precise decomposition of trimmed trivariates into tensor products. Comput. Aided Geom. Des. 71, 1–15.

Massarwi, F., Elber, G., 2016. A B-spline based framework for volumetric object modeling. Comput. Aided Des. 78, 36-47.

McDonnell, K.T., Chang, Y.S., Qin, H., 2004. Interpolatory, solid subdivision of unstructured hexahedral meshes. Vis. Comput. 20, 418-436.

McDonnell, K.T., Neophytou, N., Mueller, K., Qin, H., 2007. Subdivision volume splatting. In: EuroVis. Citeseer, pp. 139-146.

Pan, M., Chen, F., Tong, W., 2018. Low-rank parameterization of planar domains for isogeometric analysis. Comput. Aided Geom. Des. 63, 1–16.

Pan, M., Chen, F., Tong, W., 2020. Volumetric spline parameterization for isogeometric analysis. Comput. Methods Appl. Mech. Eng. 359, 112769.

Pan, Q., Xu, G., Xu, G., Zhang, Y., 2016. Isogeometric analysis based on extended Catmull-Clark subdivision. Comput. Math. Appl. 71, 105-119.

Pan, Q., Xu, G., Zhang, Y., 2014. A unified method for hybrid subdivision surface design using geometric partial differential equations. Comput. Aided Des. 46, 110–119.

Qi, D., Tian, Z., Zhang, Y., Zheng, J., 1975. The method of numeric polish in curve fitting. Acta Math. Sin. 18, 173-184.

Stam, J., 1998. Exact evaluation of Catmull-Clark subdivision surfaces at arbitrary parameter values. In: Proceedings of the ACM SIGGRAPH Conference on Computer Graphics, vol. 32, pp. 395–404.

- Wang, W., Zhang, Y., Liu, L., Hughes, T.J., 2013. Trivariate solid T-spline construction from boundary triangulations with arbitrary genus topology. Comput. Aided Des. 45, 351–360.
- Wang, W., Zhang, Y., Xu, G., Hughes, T.J., 2012. Converting an unstructured quadrilateral/hexahedral mesh to a rational T-spline. Comput. Mech. 50, 65–84. Wei, X., Zhang, Y., Hughes, T.J., Scott, M.A., 2015. Truncated hierarchical Catmull–Clark subdivision with local refinement. Comput. Methods Appl. Mech. Eng. 291, 1–20.
- Wei, X., Zhang, Y., Liu, L., Hughes, T.J., 2017a. Truncated T-splines: fundamentals and methods. Comput. Methods Appl. Mech. Eng. 316, 349-372.
- Wei, X., Zhang, Y.J., Hughes, T.J., 2017b. Truncated hierarchical tricubic C⁰ spline construction on unstructured hexahedral meshes for isogeometric analysis applications. Comput. Math. Appl. 74, 2203–2220.
- Wei, X., Zhang, Y.J., Hughes, T.J., Scott, M.A., 2016. Extended truncated hierarchical Catmull-Clark subdivision. Comput. Methods Appl. Mech. Eng. 299, 316–336.
- Wei, X., Zhang, Y.J., Toshniwal, D., Speleers, H., Li, X., Manni, C., Evans, J.A., Hughes, T.J., 2018. Blended B-spline construction on unstructured quadrilateral and hexahedral meshes with optimal convergence rates in isogeometric analysis. Comput. Methods Appl. Mech. Eng. 341, 609–639.
- Xu, G., Dong, Z., Xu, J., Wang, C., Zhang, Y., Mourrain, B., 2020. Multi-resolution spline topology optimization. Preprint.
- Xu, G., Jin, Y., Xiao, Z., Wu, Q., Mourrain, B., Rabczuk, T., 2018. Exact conversion from Bézier tetrahedra to Bézier hexahedra. Comput. Aided Geom. Des. 62, 154–165.
- Xu, G., Kwok, T.H., Wang, C.C., 2017. Isogeometric computation reuse method for complex objects with topology-consistent volumetric parameterization. Comput. Aided Des. 91, 1–13.
- Xu, G., Mourrain, B., Duvigneau, R., Galligo, A., 2013a. Analysis-suitable volume parameterization of multi-block computational domain in isogeometric applications. Comput. Aided Des. 45, 395–404.
- Xu, G., Mourrain, B., Duvigneau, R., Galligo, A., 2013b. Optimal analysis-aware parameterization of computational domain in 3d isogeometric analysis. Comput. Aided Des. 45, 812–821.
- Xu, G., Mourrain, B., Galligo, A., Rabczuk, T., 2014. High-quality construction of analysis-suitable trivariate NURBS solids by reparameterization methods. Comput. Mech. 54, 1303–1313.
- Xu, G., Mourrain, B., Wu, X., Chen, L., Hui, K.C., 2015. Efficient construction of multi-block volumetric spline parameterization by discrete mask method. J. Comput. Appl. Math. 290, 589–597.
- Zhang, Y., Bazilevs, Y., Goswami, S., Bajaj, C.L., Hughes, T.J., 2007. Patient-specific vascular NURBS modeling for isogeometric analysis of blood flow. Comput. Methods Appl. Mech. Eng. 196, 2943–2959.
- Zhang, Y., Wang, W., Hughes, T.J., 2012. Solid T-spline construction from boundary representations for genus-zero geometry. Comput. Methods Appl. Mech. Eng. 249, 185–197.
- Zhang, Y., Wang, W., Hughes, T.J., 2013. Conformal solid T-spline construction from boundary T-spline representations. Comput. Mech. 51, 1051-1059.